Crustal Deformation caused by magma migration in the northern Izu Islands, Japan

Takuya Nishimura,[1] Shinzaburo Ozawa,[1] Makoto Murakami,[1]
Takeshi Sagiya,[1] Takashi Tada,[1] Masaru Kaidzu,[1] and Motoo Ukawa[2]

Abstract. Intense crustal activity including earthquake swarms, eruptions, and a caldera formation in the northern Izu Islands started on June 26, 2000, accompanied with large crustal deformation. Permanent GPS data reveals the spatial pattern and time evolution of ground deformation. The observations reveal shrinking and subsidence of Miyakejima and extension between Kouzushima and Niijima. We constructed a source model to explain the observed displacements during the period between June 26 and the end of August. The model consists of a deflation source (0.12km^3) beneath Miyakejima, tensile faults (1.04km^3) located between Miyakejima and Kouzushima, and several shear faults. Mass balance considerations suggest that a large amount of magma migrated 30km from Miyakejima toward Kouzushima.

Introduction

The Izu Islands are a chain of volcanoes lying along the boundary between the Pacific plate and the Philippine Sea plate. Miyakejima, Kouzushima, and Niijima are located in the northern part of the Izu Islands (Figure 1) and we abbreviated them to MI, KO, and NI, respectively. Miyakejima volcano is an active stratovolcano. A total of 14 historical eruptions are documented for the past millenium [*Tsukui and Suzuki,* 1998]. Fissure eruption of basaltic lava on the flank of the volcano is the typical style of the eruptions including recent ones which occurred in 1940, 1962 and 1983. Most volcanologists anticipated a similar type of eruption would occur sooner or later because of the periodicity of the recent eruptions.

Figure 1

However, the 2000 eruption was different from previous ones in many respects. It started with shallow earthquakes in MI at a depth of ~3km at ~9:00UT on June 26, 2000 [cf. *JMA*, 2000]. At the same time, a sudden change of distances between GPS stations on MI was observed by continuous measurements. Six hours later, the hypocenters of the earthquakes moved westward to the ocean off MI. A small submarine eruption which ejected $5\times10^{-6}\text{km}^3$ occurred 1.5km off the western coast of MI at 0:00UT on June 27 [*Shirao et al.,* 2000], when the seismicity migrated through the area. The intense earthquake swarm moved further northwestward toward KO and continued near KO for ~50 days. The first eruption at the summit of Miyakejima volcano occurred on July 8. Just after this eruption, the summit collapsed and a caldera was formed. The caldera collapse continued for ~40 days during the period MI contracted significantly. The depth and diameter of the caldera reached 550m and 1600m, respectively, with collapsed volume totaling $0.6km^3$ [*Hasegawa et al.,* 2001]. Subsequently, summit eruptions occurred as tephra ejecta on July 14-15, August 9-10, 18 and 28. Total volume of erupted materials is less than $0.02km^3$ [*Nakada and Fujii,* 2000]. In mid September, the collapse caldera started emitting a large amount of volcanic gasses.

In this study, we show the crustal deformation observed at the permanent GPS sites and construct a model based on the observed displacements. The dates and times in this article are based on Universal time(UT).

Displacement Observed by GPS

GPS coordinates in this study are processed with GIPSY-OASIS II software using the precise point positioning technique [*Zumberge et al.,* 1997] and subsequently bias-fixed via double-differencing of solutions. To detect rapid deformation, we computed coordinates of the GPS sites every 6 hours using 6-hour session data.

Figure 1 shows horizontal displacements of the GPS stations located in the northern Izu Islands and its vicinity. The vectors show the differences between the average coordinates of June 13-22 and those of August 27-31. Since the plate motion for 2 months is negligible (Figure 1) , we can conclude the observed displacements are mainly caused by the 2000 Izu Islands activity. In MI, the observed displacements show radiative horizontal pattern suggesting shrinking of the island and subsidence by 80 cm. An extension between KO and NI reached ∼90cm. It should be noted that the displacement field of the 2000 episode was observed even in Boso and Izu Peninsulas, 100km away.

Figure 2 shows the temporal changes in components of selected baselines. Rapid changes of baselines 0599-3060 and 3059-0600 in MI started almost simultaneously with the earthquake swarms. The speed of the baseline changes decreased gradually during the first 10 days just after the breakout of the swarm. It is interesting to note the polarity of change in the NS and EW components of baseline 3059-0600 reversed on July 27-28. Ten days after the start of the swarm the rate of crustal deformation became almost constant and it continued at this rate until the beginning of September. There were small fluctuations from constant trend of the deformation and it seems that these are associated with the summit eruptions on MI on July 8, July 14, and August 18. A change in baseline 3057-3058 appears on June 28, as the seismicity migrated and approached KO. Rapid changes continued for ∼50 days. There are several coseismic steps associated with $\sim M6$ earthquakes in the timeseries. There were also fluctuations from the trend and those are correalated with the seismic activity.

Figure 2

Modeling

We have constructed a model for ground displacements from the 2000 Izu Islands crustal activity observed at more than 30 GPS stations in the Izu Islands and the mainland of Japan by the Geographical Survey Institute(GSI). We also used data from 3 GPS stations in MI operated by National

Research Institute for Earth Science and Disaster Prevention(NIED). In this section, we use a two step approach to derive our model. We first estimate the deformation solely caused by earthquakes. Then, we estimate displacements caused by volcanic sources.

NIED has been determining CMT(Centroid Moment Tensor) solutions for major earthquakes in and around Japan by inversion of seismic surface waves since 1997 on a routine basis [*Fukuyama et al.,* 1998]. The NIED catalog covers most earthquakes of $M_w \geq 4.0$ in the 2000 episode. The coseismic displacements of the 5 largest earthquakes are notable in the time-series of coordinates change of several GPS sites. Using a nonlinear inversion method [*Matsu'ura and Hasegawa,* 1987], we estimated fault parameters of these 5 largest earthquakes based on the coseismic displacements. We selected one of two conjugate nodal planes using the aftershock distribution. The lengths and widths of faults are assumed to satisfy empirical relations between magnitude and fault area [*Sato,* 1979]. The inverted data were the 3 components of coseismic displacements at the GPS sites, which were defined as the differences between the average of four 6-hours coordinates before and after the earthquake. Theoretical displacements were calculated by *Okada* [1992]'s formulation. Optimal fault parameters are listed in Table 1.

Table 1

In addition to the earthquakes modeled above, we calculated synthetic displacements due to 1349 point dislocation sources based on NIED's mechanism solutions and JMA's hypocenter distribution. Their moment magnitude range from 3.4 to 5.7. The synthetic displacements due to the total of 1349 point sources reach 8cm at several GPS sites. Figures 2 and 3 show synthetic time-series and cumulative displacement calculated by the 5 largest earthquakes and the 1349 point sources. The calculated coseismic displacements are much smaller than the observed ones. This discrepancy suggests that magmatic activity caused most of the observed displacements. We use the differences between the observed displacements in Figure 1 and the calculated coseismic displacements as data to invert for parameters of the aseismic sources.

Figures 2 and 3

Using the hypocenter distributions as guides we assumed the geometries of the sources as shown in Figure 4 through trial and error modeling. We, first, assumed a point deflation source [*Mogi,* 1958; *Tada and Nakamura,* 1988] beneath MI to simulate the shrinking and subsidence of MI. Second, we assumed magma (dike) intrusion in the seismicity zone expanding from MI to KO to model the extension of the baseline 3057-3058. The seismicity zone can be subdivided into two groups, the southeastern group where seismicity ceased by June 28 and the northwestern group where seismicity continued for 50 days after June 28. Precise determination of hypocenters in the northwestern group by ocean bottom seismometers [*Sakai et al.,* 2001] shows that they form a thin vertical sheet below a depth of 5km. We therefore assumed two tensile faults, adopting the geometry and locations fixed by the seismicity. Third, using only a point deflation and two tensile faults we cannot explain the dis-

Figure 4

placements in KO and NI, particularly, at 0597. Therefore, we assumed a shear fault whose mechanism is similar to those of the large earthquakes on July 1, July 8, and August 18 at the northern edge of the northern tensile fault. This is a hypothetical fault but we found that without it we cannot simulate the observed displacements. Southeastward movements in the southern Izu Peninsula support the existence of this shear fault.

Results and Discussion

Optimal fault parameters estimated using the above procedure are shown in Table 2. At MI, a point source deflated by 0.12km^3 at a depth of 4.2km, 2km south-southwest to the caldera. This is interpreted as the squeezing of magma from a magma reservoir of Miyakejima volcano. On the other hand, two tensile faults in the region between MI and KO opened by 2.3m and 7.8m, respectively. These are the intruded dikes assosiated with a large amount of magma (1.04km^3).

Table 2

The moment magnitude associated with shear faulting is estimated to be 6.6, almost equal to the total seismic moment of the earthquake swarm that occurred east KO according to NIED's catalogue. This result strongly suggests significant aseismic creep occurred near the intruded dikes. It seems that the shear faulting accompanied dike opening. However, there is no evidence that the aseismic fault motions occurred on a single fault. Slow aseismic slip and afterslip may occur on many faults which together constitute the 2000 Izu Islands earthquake swarms.

The volume of erupted materials ($<0.02\text{km}^3$) [*Nakada and Fujii,* 2000] is significantly smaller than the volume decrease of the magma reservoir (0.12km^3) and the volume of the caldera collapse (0.60km^3) [*Hasegawa et al.,* 2001] in MI. On the other hand, the volume of the intruded dikes (1.04km^3) is the same order of magnitude as the total volume decrease in MI ($\sim 0.70\text{km}^3$). This suggests that most of the collapsed materials at the summit of MI drained back through the conduit to the magma reservoir and migrated northwestward by as much as 30km in the form of a dike intrusion. The residual of 0.34km^3 could be explained by the error of our estimation caused by our idealized assumptions. However, we speculate that the residual reflects the existence of a magma reservoir system east KO.

Acknowledgments. We are grateful to Japan Meteorological Agency(JMA) and Shin-ichi Sakai of University of Tokyo for providing lists of earthquake hypocenters. Careful comments by Danan Dong, Gamel S. El-Fiky, and Wayne Thatcher improve the manuscript. We appreciate Peter C. La Femina and two anonymous reviewers for useful suggestions. We used results of earthquake mechanism analysis using broadband seismic waveforms conducted under Freesia Project, NIED.

References

Aki, K., and P. G. Richards, *Quantitative Seismology*, 932 pp., W.H. Freeman and Company, San Francisco, 1980.

Fukuyama, E., M. Ishida, D. S. Dreger, H. Kawai, Automated seismic moment tensor determination by using on-line broad-band seismic waveforms (in Japanese with English abstract), *J. Seismol. Soc. Jpn., 51*, 149-156, 1998.

Hasegawa, H., M. Murakami, K. Matsuo, Caldera subsidence measurement at Miyakejima summit (in Japanese), *J. Geog. Surv. Inst., 95,* 121-128, 2001.

Japan Meteorological Agency, Recent seismic activity in the Miyakejima and Niijima-Kozushima region, Japan - the largest earthquake swarm ever recored, *Earth Planets Space, 52,* i-viii, 2000.

Matsu'ura, M., and Y. Hasegawa, A maximum likelihood approach to nonlinear inversion under constraints, *Phys. Earth Planet. Inter., 47,* 179-187, 1987.

Mogi, K., Relations between the eruptions of various volcanoes and the deformations of the ground surfaces around them, *Bull. Earthq. Res. Inst., Univ. Tokyo, 36,* 99-134, 1958.

Nakada, S., T. Fujii, Sequence and interpretation of caldera-forming event at Miyakejima Volcano, Japan, *Eos Trans. AGU, 81*(48), Fall Meet. Suppl., Abstract V52A-02, 2000.

Okada, Y., Internal deformation due to shear and tensile faults in a half-space, *Bull. Seismol. Soc. Am., 82,* 1018-1040, 1992.

Sakai, S.,*et. al.*, Hypocenter distribution in and around the Izu volcanic islands in 2000 (in Japanese with English abstract), *J. Geog. 110*, 145-155, 2001.

Sato, R., Theoretical basis on relationships between focal parameters and earthquake magnitude, *J. Phys. Earth, 27,* 353-372, 1979.

Shirao, M.,*et. al.*, Submarine observation of undersea craters in Miyake-jima 2000 eruption (abstract in Japanese), Prog. Abst. Volcano. Soc. Jpn., 5, 2000.

Tada, T., and K. Nakamura, M., Inflation-deflation related with the 1983 eruption of Miyakejima Volcano, Japan (in Japanese with English abstract), *Bull. Volcano. Soc. Jpn., 33,* 173-184, 1988.

Tsukui, M., and Y. Suzuki, Eruptive history of Miyakejima Volcano during the last 7000 years (in Japanese with English abstract), *Bull. Volcano. Soc. Jpn., 43,* 149-166, 1998.

Zumberge, J. F., M. B. Heflin, D. C. Jefferson, M. M. Watkins, and F. H. Webb, Precise point positioning for the efficient and robust analysis of GPS data from large network, *J. Geophys. Res., 102,* 5005-5017, 1997.

M. Kaidzu, M. Murakami, T. Nishimura, S. Ozawa, T. Sagiya, and T. Tada, Geographical Survey Institute, Kitasato-1, Tsukuba, 305-0811, Japan. (e-mail: t_nisimura@gsi.go.jp)

M. Ukawa, National Research Institute for Earth Science and Disaster Prevention, Tennodai 3-1, Tsukuba, 305-0006, Japan. (e-mail: ukawa@bosai.go.jp)

(Received February 20, 2001; revised May 17, 2001; accepted June 27, 2001.)

---

[1]Geographical Survey Institute, Tsukuba, Japan

[2]National Research Institute for Earth Science and Disaster Prevention, Tsukuba, Japan

Figure 1. Horizontal displacements at GEONET GPS stations during the period from June 13-22 to August 27-31. Stars show epicenters of the 5 largest earthquakes (M_{JMA} ≥6.0) in the episode [*JMA*, 2000]. Four digit number represents a station code of selected GPS stations. Abbreviation in tectonic map (inset): NA; North American plate; PA, Pacific plate; PH, Philippine Sea plate; AM, Amurian plate.

Figure 1. Horizontal displacements at GEONET GPS stations during the period from June 13-22 to August 27-31. Stars show epicenters of the 5 largest earthquakes (M_{JMA} ≥6.0) in the episode [*JMA*, 2000]. Four digit number represents a station code of selected GPS stations. Abbreviation in tectonic map (inset): NA; North American plate; PA, Pacific plate; PH, Philippine Sea plate; AM, Amurian plate.

Figure 2. Time series of 6-hours coordinates in selected GPS baselines. Arrows indicate the onsets of eruptions of Miyakejima volcano and major earthquakes. Solid lines show the synthetic time series of the modeled earthquakes. (a) coordinate changes of 3060 relative to 0599. (b) coordinate changes of 0600 relative to 3059. (c) coordinate changes of 3058 relative to 3057.

Figure 2. Time series of 6-hours coordinates in selected GPS baselines. Arrows indicate the onsets of eruptions of Miyakejima volcano and major earthquakes. Solid lines show the synthetic time series of the modeled earthquakes. (a) coordinate changes of 3060 relative to 0599. (b) coordinate changes of 0600 relative to 3059. (c) coordinate changes of 3058 relative to 3057.

Figure 3. Calculated coseismic displacements and the modeled fault. Arrows mean the calculated displacements at the permanent GPS stations of GSI and NIED. Rectangles and stars are the fault planes and epicenters of the 5 largest earthquakes, respectively. The solid lines of the rectangles mean their upper sides. Gray circles represent locations of point dislocation sources corresponding to the major earthquakes except for the 5 largest ones.

Figure 3. Calculated coseismic displacements and the modeled fault. Arrows mean the calculated displacements at the permanent GPS stations of GSI and NIED. Rectangles and stars are the fault planes and epicenters of the 5 largest earthquakes, respectively. The solid lines of the rectangles mean their upper sides. Gray circles represent locations of point dislocation sources corresponding to the major earthquakes except for the 5 largest ones.

Figure 4. Optimal fault model and horizontal displacements. White and black arrows mean calculated displacements and inversion data defined as the differences between the observed displacements and the synthetic coseismic displacements. Gray circles are epicenters of the earthquake of $M_{JMA} \geq 3.5$ [*JMA*, 2000].

Figure 4. Optimal fault model and horizontal displacements. White and black arrows mean calculated displacements and inversion data defined as the differences between the observed displacements and the synthetic coseismic displacements. Gray circles are epicenters of the earthquake of $M_{JMA} \geq 3.5$ [*JMA*, 2000].

Table 1. The fault parameters of the 5 largest earthquakes

Origin time (UT)	NIED M_w	Lat.(°N)	Lon.(°E)	Depth (km)	Length (km)	Strike(°)	Dip(°)	Rake(°)	Slip(m)
2000/7/1 7:01	6.2	34.210 (0.016)	139.208 (0.019)	0.1 (0.9)	**15.8**	**100**	**41**	**204**	1.44 (0.48)
2000/7/8 18:57	5.9	34.226 (0.009)	139.225 (0.019)	3.2 (3.0)	**11.2**	**95**	**48**	**208**	0.91 (0.24)
2000/7/15 1:30	6.0	34.437 (0.011)	139.162 (0.018)	**1.0**	**12.6**	**107**	**82**	**193**	0.39 (0.09)
2000/7/30 12:25	6.4	33.872 (0.016)	139.386 (0.018)	2.3 (0.9)	**20.0**	**11**	**85**	**347**	1.11 (0.19)
2000/8/18 8:02	5.7	34.234 (0.010)	139.178 (0.012)	1.0 (0.8)	**8.9**	**90**	**74**	**177**	0.42 (0.14)

Bold numbers represent fault parameters fixed values in inversion. Values in the parenthese are 1σ. The locations of the faults are represented in the convention of *Aki and Richards* [1980]. Fault widths are a half of lengths.

Table 2. The parameters of aseismic sources

Source Type (°N)	Lat. (°E)	Lon.	Depth (km)	Length (km)	Width (km)	Strike (°)	Dip (°)	Rake (°)	Open (m)	Slip (m)	Volume Change(km^3)
Deflation	34.067 (0.0002)	139.521 (0.0004)	4.2 (0.1)	-	-	-	-	-	-	-	-0.12 (0.03)
Tensile fault A	**34.137**	**139.373**	0.5 (0.1)	**12.7**	**10.0**	**125**	**77**	-	2.3 (0.1)	-	0.29
Tensile fault B	**34.225**	**139.254**	6.3 (0.4)	**14.5**	6.7 (0.9)	**128**	**90**	-	7.8 (1.0)	-	0.75
Shear fault	**34.225**	**139.254**	2.4 (0.3)	4.3 (0.3)	8.1 (1.5)	290 (1)	**90**	165 (2)	-	10.0 (2.2)	-

Bold numbers represent fault parameters fixed values in inversion. Values in the parenthese are 1σ. The locations of the faults are represented in the convention of *Aki and Richards* [1980].

NISHIMURA ET AL.: MAGMA MIGRATION IN NORTHERN IZU ISLANDS

NISHIMURA ET AL.: MAGMA MIGRATION IN NORTHERN IZU ISLANDS

NISHIMURA ET AL.: MAGMA MIGRATION IN NORTHERN IZU ISLANDS

NISHIMURA ET AL.: MAGMA MIGRATION IN NORTHERN IZU ISLANDS

NISHIMURA ET AL.: MAGMA MIGRATION IN NORTHERN IZU ISLANDS

NISHIMURA ET AL.: MAGMA MIGRATION IN NORTHERN IZU ISLANDS

NISHIMURA ET AL.: MAGMA MIGRATION IN NORTHERN IZU ISLANDS

NISHIMURA ET AL.: MAGMA MIGRATION IN NORTHERN IZU ISLANDS

NISHIMURA ET AL.: MAGMA MIGRATION IN NORTHERN IZU ISLANDS

NISHIMURA ET AL.: MAGMA MIGRATION IN NORTHERN IZU ISLANDS

NISHIMURA ET AL.: MAGMA MIGRATION IN NORTHERN IZU ISLANDS

NISHIMURA ET AL.: MAGMA MIGRATION IN NORTHERN IZU ISLANDS

NISHIMURA ET AL.: MAGMA MIGRATION IN NORTHERN IZU ISLANDS

NISHIMURA ET AL.: MAGMA MIGRATION IN NORTHERN IZU ISLANDS

NISHIMURA ET AL.: MAGMA MIGRATION IN NORTHERN IZU ISLANDS

NISHIMURA ET AL.: MAGMA MIGRATION IN NORTHERN IZU ISLANDS

NISHIMURA ET AL.: MAGMA MIGRATION IN NORTHERN IZU ISLANDS

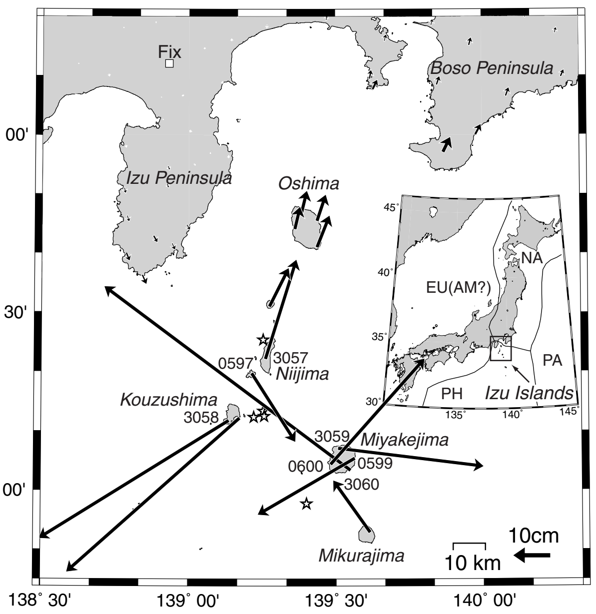
Fix
Boso Peninsula
35° 00'
Izu Peninsula
Oshima
EU(AM?)
NA
PA
PH
Izu Islands
34° 30'
0597
3057
Niijima
Kouzushima
3058
3059
Miyakejima
0600
0599
3060
34° 00'
Mikurajima
10 km
10cm
138° 30'
139° 00'
139° 30'
140° 00'

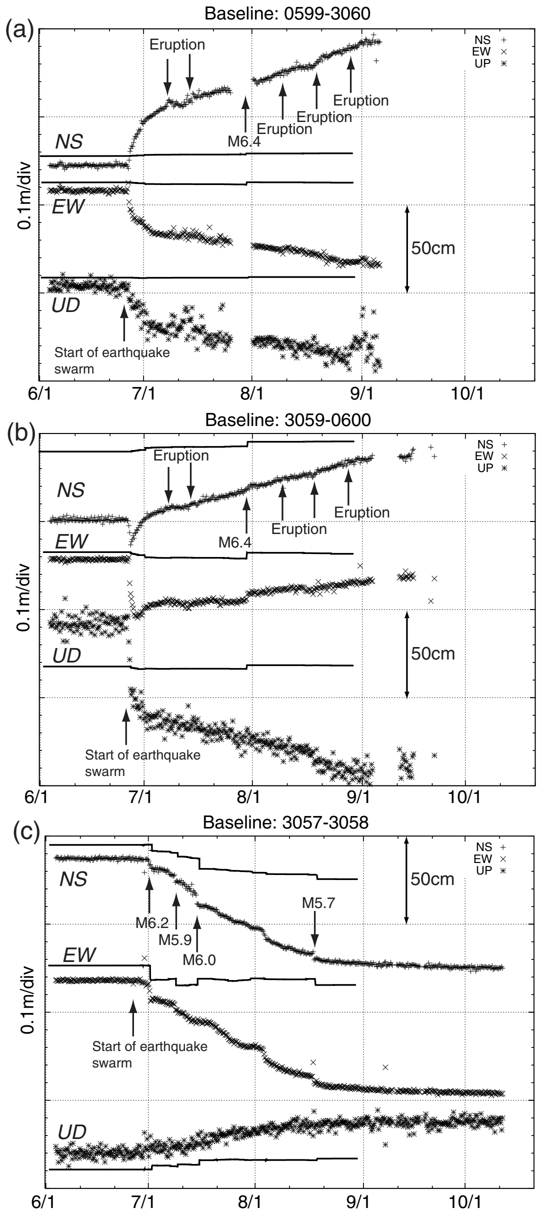

(a)
Baseline: 0599-3060
NS
EW
UP
Eruption
Eruption
Eruption
Eruption
M6.4
NS
EW
UD
0.1m/div
50cm
Start of earthquake swarm
6/1
7/1
8/1
9/1
10/1
(b)
Baseline: 3059-0600
NS
EW
UP
Eruption
Eruption
Eruption
M6.4
NS
EW
UD
0.1m/div
50cm
Start of earthquake swarm
6/1
7/1
8/1
9/1
10/1
(c)
Baseline: 3057-3058
NS
EW
UP
NS
M6.2
M5.9
M6.0
M5.7
EW
UD
0.1m/div
50cm
Start of earthquake swarm
6/1
7/1
8/1
9/1
10/1

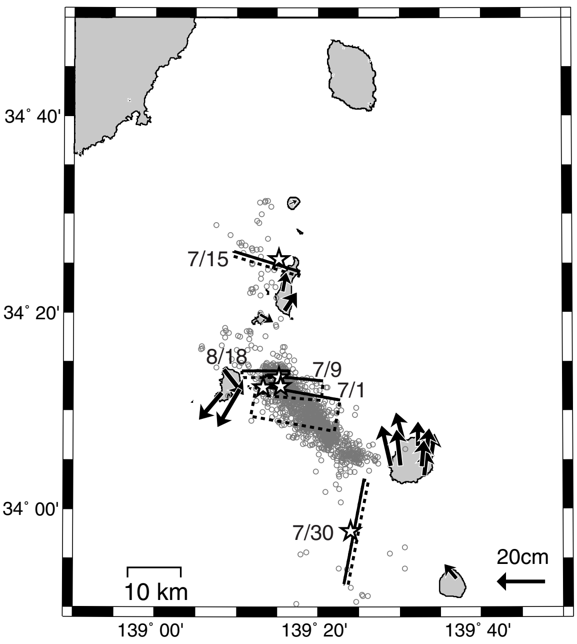

34° 40'
34° 20'
34° 00'
139° 00'
139° 20'
139° 40'
7/15
8/18
7/9
7/1
7/30
10 km
20cm

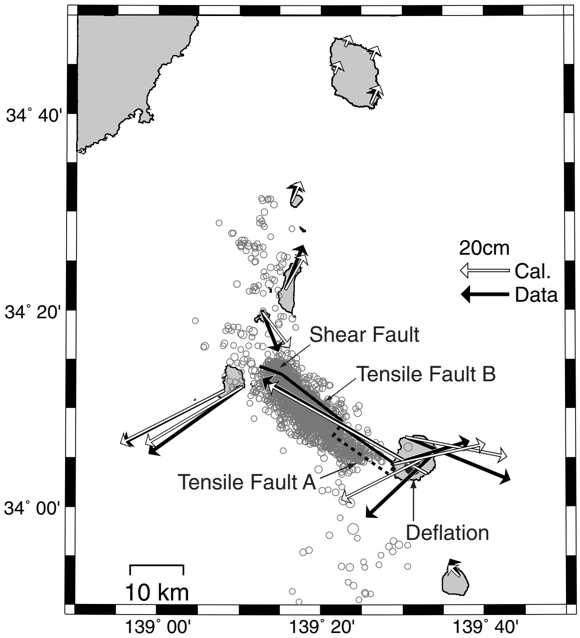
34° 40'
34° 20'
34° 00'
139° 00'
139° 20'
139° 40'
20cm
Cal.
Data
Shear Fault
Tensile Fault B
Tensile Fault A
Deflation
10 km